Extended Materials and Methods

Cells

Rat amniotic fluid stem cells (rAFSCs) were isolated from amniotic fluid of E12 Sprague-Dawley rat fetuses as described (*66*), and grown in alpha-Minimal Essential Media (αMEM, Gibco, ThermoFisher) supplemented with 20% Chang supplements (Irvine Scientific), 15% fetal bovine serum (FBS, ThermoFisher Scientific), and 0.5% Penicillin/Streptomycin (ThermoFisher Scientific). Human AFSCs (hAFSCs) were obtained under good manufacturing practice guidelines as described (UCL/UCLH REC Reference: 08/0304) (*22*). Sprague-Dawley rat bone-marrow derived mesenchymal stem cells (MSCs) were purchased (CellBiologics) and grown in supplier recommended medium until 90% confluence. Human adenocarcinomic alveolar basal epithelial cells (A549) were purchased (Sigma Aldrich) and grown in Dulbecco's Modified Eagle Medium, (DMEM) with Nutrient Mixture F-12 media (Gibco, ThermoFisher) supplemented with 10% FBS and 0.5% Penicillin/Streptomycin. All cells were used within 6 passages. Human pulmonary alveolar epithelial cells (HPAEpiC) were obtained from the lungs of a healthy fetus at 21 weeks of gestation (ScienCell), grown in supplier recommended medium, and used immediately for proliferation and viability assays. Human bone marrow-derived MSCs were obtained from a healthy donor (ATCC) and grown in supplier recommended medium. Human MSCs were used within three passages.

Extracellular vesicles (EVs)

EVs from rat and human AFSCs and from MSCs were isolated by ultracentrifugation from cells that were treated with exosome-depleted FBS (ThermoFisher) for 18 h, as described (*29*). Based on previous studies and confirmed in this study, we established that $4x10^6$ AFSCs cultured under

these conditions secrete approximately $3x10^9 \pm 1x10^7$ EVs, as quantified by nanoparticle tracking analysis (*29*). For all in vitro, ex vivo, and in vivo experiments herein described, we administered 50 µL of the EV preparation that corresponds to 0.5% of the conditioned medium (50 µL EV volume of 10 mL CM volume, v/v) and $1.5x10^8 \pm 5x10^5$ EVs. For in vitro organoid experiments, the dose was $3.6x10^8 \pm 1.2x10^6$ EVs.

EVs used in this study were characterized for size by nanoparticle tracking analysis, morphology by transmission electron microscopy, and expression of canonical EV-related markers by Western blot (fig. S1), as described (*29*) and recommended by the International Society for Extracellular Vesicles. Small EVs had a mean size of 140 ± 5 nm and mode size 104 ± 11 nm. To isolate medium/large EVs (m/lEVs, >200 nm), sucrose gradient ultracentrifugation was used with six layers ranging from 10% to 90% sucrose in phosphate-buffered saline (PBS). rAFSC-CM was spun through this gradient at 100,000 g for 14 h. Fractionated layers were isolated and nanoparticle tracking analysis was used to confirm the presence of large vesicles (m/lEVs mean size of 363 ± 17 nm, mode size 217 ± 32 nm).

Ex vivo model of pulmonary hypoplasia

In fetal rats, pulmonary hypoplasia was induced as described (*30, 40*) with the administration of nitrofen (Sigma Aldrich) to pregnant Sprague-Dawley rats (100 mg in 1 mL olive oil; protocol #39168, #49892). At E14.5, the dam was euthanized, and fetal lungs were harvested. Lungs were washed in PBS, grown on 0.8 µm nanofilter membranes, and incubated for 72 h in culture medium alone (DMEM), rAFSC-CM, or medium supplemented with rAFSC-EVs or rMSC-EVs (0.5% v/v). For AFSC co-culture experiments, five thousand rAFSCs were seeded onto the bottom of the plate, and lung explants on nanofilter membranes were added on top of the cells and allowed to float for 72 h. Fetal lungs from dams that received olive oil (no nitrofen) at E9.5 served as control.

In vitro model of pulmonary hypoplasia

At E14.5, a single cell suspension was obtained from pooled lungs of control or nitrofen-injured rat fetuses by trypsinization (0.25% Trypsin-EDTA, ThermoFisher) for 20 minutes. Cells were spun down by centrifugation (5 minutes, 800 g) and the pellet was resuspended in DMEM supplemented with 10% FBS and subjected to three serial depletions of fibroblasts by incubation for 1 h each following an established protocol (*40, 62*). Cells were used to test epithelial homeostasis and to generate fetal lung organoids for assessment of epithelial cell differentiation. For epithelial homeostasis experiments, cells were grown for 5 days in Bronchial Epithelial Cell Growth Medium (BEGM; Lonza). Cells were checked daily for proper epithelial morphology using a light microscope. On the fifth day, cells were confirmed to be positive for SPC and negative for vimentin via immunofluorescence staining assays. Epithelial homeostasis was investigated by assessing cell proliferation and cell death as described (*40*) on cells from nitrofen-injured lungs that either had their medium replaced with BEGM, or BEGM supplemented with 500 µL of rAFSC-CM, 500 µL of EV-depleted rAFSC-CM, rAFSC-EVs, or rMSC-EVs (0.5% v/v). For AFSC co-culture experiments, rAFSCs were seeded in the top compartment of a transwell (0.4 µm) and primary lung epithelial cells were seeded in the bottom compartment (in a ratio of 1:10, rAFSC to primary lung epithelial cells), as described (*40*).

For epithelial differentiation experiments, cells were seeded in a ratio of 60:40 semi-solid Matrigel (Corning) to medium ratio, to generate organoids as described (*63*). Cells from nitrofen-injured fetuses were cultured for 10 days with medium alone or with medium supplemented with 1.2% v/v rAFSC-EVs or rMSC-EVs. Lung organoids from untreated fetuses served as control. Medium was replaced every other day.

Human A549 cells were injured for 24 h with nitrofen (40 μM), and subsequently administered medium alone, hAFSC-EVs or hMSC-EVs (0.5% v/v). Untreated and uninjured A549 cells served as control. Following 24 h incubation, proliferation and cell death rates were determined by EdU incorporation kit (Click-IT, ThermoFisher Scientific), and Live/Dead cell viability assay (ThermoFisher Scientific), as described (*40*). Experiments were repeated for control (n=4), medium only (n=4), hAFSC-EVs (n=4), hMSC-EVs (n=4), and included >30 technical replicates.

HPAEpiC from a fetus at 21 weeks of gestation contained both alveolar type I and type II cells, which were selected with cytokeratin-18 and cytokeratin-19 by the supplier. Cells were grown in supplier recommended medium and used in the first passage after reaching ~70% confluence. HPAEpiC were stressed with nitrofen exposure at 400 μm (dosage at 40 μm was not optimal in inducing impairment in cell proliferation or viability). Experiments were repeated for control (n=6), medium only (n=6), hAFSC-EVs (n=4), hMSC-EVs (n=4), and included >100 technical replicates.

In vivo model of pulmonary hypoplasia

In fetal rabbits, pulmonary hypoplasia was induced secondary to surgical creation of a diaphragmatic hernia at embryonic day E25 in New Zealand rabbits, following ethical approval (protocol #191/2018, #40/2020), as described *(41*). Two days later at E27, tracheal ligation was performed either alone or in conjunction with EV administration [rAFSC-EVs (n=9), rMSC-EVs (n=8), or hAFSC-EVs (n=5)]. EVs (50 μL) were injected intra-tracheally prior to ligation of the trachea as shown in Movie S6. Lungs were harvested at E31 and immediately frozen for RNA extractions or were fixed in 4% paraformaldehyde and embedded in paraffin. Fetal rabbits with intact diaphragms and that did not receive tracheal occlusion served as control.

Lung morphometry

In fetal rats, lung explants from different conditions were compared for terminal bud density and surface area using ImageJ independently by two blinded researchers, as described (*27*). Terminal branching was measured by counting the number of terminal buds defined as the number of single acini separated by distinct septae at the periphery of the explant (*27*). Differential interference contrast photos were taken on a light microscope (Leica DMI6000B) at 2.5X magnification. Experiments were repeated as many times as indicated: control (n=16), medium only (n=17), rAFSC-CM (n=12), medium supplemented with 0.5% v/v rAFSC-EVs (n=12), EV-depleted rAFSC-CM (n=5), RNase-treated rAFSC-EVs (n=4), rMSC-EVs (n=8), medium supplemented with 0.25% v/v rAFSC-EVs AFSC-EVs (n=5), medium supplemented with 0.05% v/v rAFSC-EVs (n=5), rAFSC-m/lEVs (n=4), and co-cultured rAFSCs (n=7).

Rabbit fetal lungs were blindly evaluated with histology (hematoxylin and eosin stain staining) to assess the number of alveoli and the thickness of the alveolar wall, as measures of the degree of lung alveolarization. For the number of alveoli, the radial alveolar count (RAC), a well-established index of alveolar number within the acinus (*64*), was determined in at least 12 counts per fetal lung in 2 different sections of the lung. For the thickness of the alveolar wall, the mean wall transection length was measured in 10 different areas of each lung, as described (*65*).

RNA expression

Lung explants from fetal rats and freshly harvested lungs of fetal rabbits were frozen at -20 °C. Total RNA was isolated using Trizol reagent (ThermoFisher Scientific), following supplier recommended protocols. Purified RNA was quantified using a NanoDrop spectrophotometer (ThermoFisher Scientific) and cDNA synthesis was performed with 200 ng for rat and 1 µg for rabbit quantified RNA (superscript VILO cDNA synthesis kit, ThermoFisher Scientific). qPCR experiments were conducted with SYBR Green Master Mix (Wisent) for 40 cycles (denaturation:

95 °C, annealing: 58 °C, extension: 72 °C) using the primer sequences reported in table S6. Melt curve plots were used to determine target specificity of the primers. ΔΔCT method was used to determine normalized relative gene expression.

To determine the expression of specific miRNAs in EVs and parent cells, RNA was extracted from approximately 4 million cells of rAFSCs and rMSCs (n=3 replicates each) using the Nucleospin miRNA kit (Macherey-Nagel), following supplier recommended protocols. EV RNA was isolated using the same procedure, from CM of the corresponding parent cells (n=3 replicates each). cDNA was synthesized using miRCURY LNA RT kit (Qiagen) and UniSp6 RNA Spike-in controls were used. Expression of miR-17-5p (YP02119304), miR-18a-5p (YP00204207), miR-19b-3p (YP00204450), miR-20a-5p (YP00204292), and controls Rnu5g (YP00203908) was assessed with miRCURY LNA SYBR Green PCR Kit (Qiagen), following supplier recommended protocols. 40-cycle qPCR was conducted as described above, and ΔΔCT method was used to determine normalized relative miRNA expression of rAFSC-EVs and rAFSCs to rMSCs and rMSC-EVs.

Immunofluorescence

Rat lung explants were fixed using 4% paraformaldehyde for 18 h, washed in PBS, and incubated in 30% sucrose for at least 18 h. Optimal cutting temperature compound (Electron Microscopy Sciences) embedded lungs were cryosectioned in coronal orientation and stained with primary antibodies reported in table S7. Fetal lung organoids were fixed in 4% paraformaldehyde for 30 minutes, permeabilized in 0.5% triton X (Sigma Aldrich) and 0.05% Tween-20 (Sigma Aldrich) in PBS, pre-blocked in 1% bovine serum albumin (BSA; Sigma Aldrich) with 0.2% triton-X and 0.05% Tween-20 in PBS. Organoids were stained with primary antibodies reported in table S7. A Leica SP8 lightning confocal microscope was used to image samples using the same laser power and exposure across conditions. Wherever possible, z-stacks were taken to increase coverage of

tissues. Total corrected cellular fluorescence was calculated to compare the fluorescence intensities between conditions, as described (*67*) using ImageJ 1.51.

Proliferation and apoptosis experiments on lung explants

Proliferation experiments in explants were conducted with the addition of EdU (10 μM final concentration in medium) to lung explants cultures 3 h prior to the 72 h endpoint of experiments. Explants were then fixed and processed for immunofluorescence assays as stated above. The Click-iT protocol was used to label EdU^+ cells (2.4:1000, Alexa Fluor 647) in co-staining experiments with SOX9 (1:1000, Alexa Fluor 488), as recommended by the supplier. Lung explants from n=4 biological replicates were used in at least triplicate technical replicates for analysis. Quantification of EdU signal was conducted with HistoQuant in QuantCenter Imaging Software (3D Histech) and covered >100 50x50 μm fields.

Cell apoptosis experiments on lung explants were conducted with the Click-iT TUNEL assay for in situ apoptosis detection, according to manufacturer's protocol. Briefly, cryo-sectioned lung explants from n=4 biological replicates were used in at least triplicate technical replicates for analysis. Alexa Fluor 647 was used in co-staining experiments. Quantification of TUNEL signal was conducted with HistoQuant in QuantCenter Imaging Software (3D Histech) and covered >100 50x50 μm fields.

Protein expression

Protein from lung explants was isolated by re-suspending explants in cell extraction buffer (ThermoFisher Scientific) supplemented with protease inhibitors (Sigma Aldrich), and sonicating for 3 cycles of 10 seconds each. Protein was quantified using the Pierce Bradford Assay (ThermoFisher Scientific), and 20 μg of protein from each sample was processed as described (*29*)

and probed for SPC and SOX9 (table S7; Data file S5). Expression of canonical EV markers CD63, Hsp70, Flo-1, and TSG101 in rAFSC-EVs and rMSC-EVs, and the nuclear marker H3K27me3 that indicates cellular debris, were analyzed as described (*29*). EV preparations did not have expression of H3K27me3, demonstrating that the preparations are free of cell debris. All details for the antibodies are available in table S7.

EV characterization and staining

To track EV migration into primary lung epithelial cells and lung explants, EV cargoes were fluorescently labelled for RNA and protein using Exo-Glow (System Biosciences) and for lipid membrane using PKH26 red fluorescent cell linker (Sigma Aldrich) following supplier recommended protocols. For PKH26 staining, EVs isolated using ultracentrifugation were re-suspended in Diluent C, stained with PKH26 for five minutes with periodic mixing, then the reaction was stopped with 1% BSA in water. Starting samples containing water only were used as negative controls for staining procedures. For live cell tracking, cells were grown on 35 mm μ-Dish plates for 24 h to reach 60% confluence (Ibitreat). DAPI was added in culture medium for 10 minutes (2% in medium), and then 2 μg of EVs stained with ExoGlow RNA or ExoGlow Protein were added and imaged once every two seconds for 10 minutes using a Leica SP8 lightning confocal microscope. After live cell imaging was performed, cells were washed twice with PBS and fixed in 4% PFA, and re-imaged to visualize the internalization of the stained EVs.

Role of rAFSC-EV RNA Cargo

To determine the role of RNA in rescuing pulmonary hypoplasia, rAFSC-EVs were treated with RNase-A (ThermoFisher) at 2 μg/μL for 90 minutes, then with RNase inhibitor (ThermoFisher) as described (*68*). Data shown in viability and proliferation assays are representative of n=3 technical replicates, with at least 5 fields per experiment. Bioanalyzer analysis (Agilent Technologies) was

used to test effectiveness of RNA degradation, after total RNA isolation using miRvana miRNA isolation kit as described above. Untreated EVs that were exposed to all temperature changes without the addition of RNase-A were used as control.

To confirm the entry of RNase into rAFSC-EVs, TSG101 and RNase were probed by immuno-EM labelling. Samples were prepared for TEM following established protocols (*29*). Briefly, fixed EV preparations (rAFSC-EVs or RNase-treated rAFSC-EVs) were allowed to absorb onto charged EM grids for 1 h. All reagents were pre-filtered using 0.22 μm syringe filters. Samples were washed in PBS, permeabilized in 0.05% triton-X in PBS for 30 minutes, washed five times in PBS, and then incubated for 2 h in primary antibody (1:100 in 10% BSA-c; Aurion) with TSG101, RNase, or both (table S7). Following five washes in PBS, samples were incubated for 1 h with the corresponding secondary antibodies (1:25 in 10% BSA-c, table S7), washed an additional five times in PBS, then fixed in 1% glutaraldehyde for 10 minutes. Following ten washes in distilled water, grids were contrasted and embedded in uranyl oxalate for 10 minutes, methyl cellulose-uranyl acetate for 10 minutes, and then prepared for EM imaging on a Tecnai 20 (FEI) from 25 kx to 100 kx magnification. Four biological replicates of rAFSC-EV-RNase and rAFSC-EVs, which included four technical replicates each, were included in these experiments. Experimental groups included single stains, and only secondary antibody stains (incubation with serum alone). Experiments were optimized for incubation time and antibody concentrations. Gold tags were identified and measured manually using the Tecnai 20 Software.

To determine if there was a carry-over effect of the RNase-A treatment on rAFSC-EVs, we performed an additional step and separated the enzymatically treated rAFSC-EVs from the supernatant, which presumably contained the inactivated RNase-A. This supernatant was then

administered to the control primary lung epithelial cells, and proliferation rate was determined as described above.

Profiling of rAFSC-EVs and rMSC-EVs

10 mL of rAFSC-CM or rMSC-CM was centrifuged at 1500 g for 5 min to remove residual cells and debris. The supernatant was transferred to a new 50 mL conical tube for EV isolation. Isolations were conducted in triplicate. ExoQuick-TC (System Biosciences) was added to the supernatant at 1:5 ratio (ExoQuick:Supernatant), mixed gently, and allowed to incubate for 18 h at 4 °C. After 24 h, the admixture was centrifuged at 1500 g for 30 min to separate EVs.

Proteomic profiling of EV cargo

EVs were quantified for protein concentration using Qubit fluorometry (Invitrogen). 10 μg of EV protein was processed by SDS-PAGE using 10% Bis Tris NuPage mini-gel (Invitrogen) in the MES buffer system. The migration window (2 cm lane) was excised and in-gel digestion was performed using a ProGest robot (DigiLab) with the following protocol: 1) Washed with 25 mM ammonium bicarbonate followed by acetonitrile. 2) Reduced with 10 mM dithiothreitol at 60 °C followed by alkylation with 50 mM iodoacetamide at room temperature. 3) Digested with trypsin (Promega) at 37 °C for 4 h. 4) Quenched with formic acid and the supernatant was analyzed directly without further processing.

The digested protein samples were analyzed by nanoscale liquid chromatography coupled to tandem mass spectrometry (MS) with a Waters NanoAcquity High Performance Liquid Chromatography system interfaced to a ThermoFisher Q Exactive. Peptides were loaded on a trapping column and eluted over a 75 μm analytical column at 350 nL/min using a 2 h reverse phase gradient; both columns were packed with Luna C18 resin (Phenomenex). The mass

spectrometer was operated in data-dependent mode, with the Orbitrap operating at 60,000 and 17,500 full width at half maximum for MS and MS/MS respectively. The fifteen most abundant ions were selected for MS/MS. Data were searched using Mascot, and parsed into Scaffold (Proteome Software) for validation, filtering and to create a non-redundant list per sample. Data was filtered using 1% protein and peptide false discovery rate (FDR) and required at least two unique peptides per protein. A minimum of three spectral count values greater than 0 in at least one of the groups was considered significantly different, and a t-test was performed on these values. For protein pathway enrichment analysis, 222 proteins that were differentially expressed in rAFSC-EVs were used as input for g:Profiler, and R package "ggplot2" was used to plot the top significantly enriched pathways for Biological Processes, Cellular Component, and Molecular Functions.

RNA-sequencing of EV cargo

Total RNA was isolated using the SeraMir Exosome RNA Purification Column kit (System Biosciences) according to the manufacturer's instructions. For each sample, 1 μL of the final RNA eluate was used for measurement of small RNA concentration by Agilent Bioanalyzer Small RNA Assay using Bioanalyzer 2100 Expert instrument (Agilent Technologies).

Small RNA libraries were constructed with the CleanTag Small RNA Library Preparation Kit (TriLink) according to the manufacturer's protocol. The final purified library was quantified with High Sensitivity DNA Reagents (Agilent Technologies) and High Sensitivity DNA Chips (Agilent Technologies). The libraries were pooled, and the 140 base pair to 300 base pair region was size selected on an 8% TBE gel (Invitrogen). The size selected library is quantified with High Sensitivity DNA 1000 Screen Tape (Agilent Technologies), High Sensitivity D1000 reagents (Agilent Technologies), and the TailorMix HT1 qPCR assay (SeqMatic), followed by a NextSeq

High Output single-end sequencing run at SR75 using NextSeq 500/550 High Output v2 kit (Illumina) according to the manufacturer's instructions.

Following an initial quality assessment with bioinformatics tool FastQC, n=3 biological replicates of rAFSC-EVs and n=2 biological replicates of rMSC-EVs were included in the final analysis. Bowtie2 was used to map the spike-in DNA, and the reads were trimmed and filtered to improve the quality of data input for read mapping using open-source tools (FastqMcf, cutadapt, PRINSEQ). After trimming, reads were mapped using open-source software (Bedtools/SAMtools). DESeq was used for differential expression analysis with default settings.

Primary Lung Epithelial Cell RNA-sequencing Experiments

Primary lung epithelial cells from nitrofen-injured lungs and normal control lungs were isolated as described above, grown in PneumaCult Ex Plus Medium, and treated with medium supplemented with rAFSC-EVs or rMSC-EVs (0.5% v/v). Total RNA extraction was conducted on n=6 biological replicates of each condition. RNA was extracted using Nucleospin miRNA kit (Macherey-Nagel) following supplier recommended protocols. Purified RNA was quantified using NanoDrop, and Bioanalyzer was used to assess the quality of RNA. Samples with RNA integrity number of > 9 were used to construct libraries. For library construction, we used an automated NEBNext Ultra II Directional with polyA isolation (New England BioLabs) using the Agilent NGS Workstation (Agilent Technologies) as per manufacturer's protocol. Briefly, 250 ng of total RNA spiked-in with SIRVs (Spike-in RNA Variant Control Mixes, Set3, Lexogen) as per manufacturer's protocol was used to generate complementary DNA (cDNA). cDNA was amplified with 12 PCR cycles. The resulting libraries were quantified with Qubit DNA HS (ThermoFisher). Fragment sizes were analyzed on the Agilent Bioanalyzer using the High Sensitivity DNA assay prior to sequencing. Paired-end sequencing was performed by The Centre for Applied Genomics,

The Hospital for Sick Children, Toronto, Canada on a NovaSeq 6000 S2 flowcell (Illumina) with a read length of 100 base pairs. 25-35 million paired end reads were obtained for each library. Sequencing quality was examined using FastQC and qualimap (see data file S2 for detailed QC metrics on sequencing libraries). Reads were aligned to the rat genome (rnor6, obtained from UCSC genome browser database) using a splice aware aligner, STAR (version 2.5.1b) with default settings. Reads were assigned to genes using featureCounts (version 1.5.3) with parameters "-p –B –s 2 –Q 255". Gene models were obtained from Ensembl (Rnor_6.0.91). Reads from ERCC (External RNA Controls Consortium, Ambion) spike-ins (included in SIRV Set3) were only used for QC purposes. For each sample, a linear model was fitted between log2 reads per million mapped reads (RPKM) values and log2 expected RNA amount of the ERCC transcripts to evaluate the accuracy of the RNA-seq measurement. Number of ERCC transcripts detected (transcripts per million > 0) and the corresponding R^2 values from the linear models are listed in data file S2. Normalized gene counts (RPKM) were calculated with R package "edgeR" (version 3.26.5) with "calcNormFactors" and "rpkm" functions. Only genes with RPKM > 1 in at least 12 samples were used for downstream analyses. All samples were used in the model fitting and dispersion estimation steps. The Quasi-likelihood F-test method was then used to identify the differentially expressed genes between pairs of conditions of interest (FDR < 0.1). Heatmaps were generated with R package "pheatmap with colors representing row-scaled RPKM values. R package "fgsea' was used for GSEA analysis. For each pair-wise comparison, genes are ranked based on their fold changes (NA vs. N or NM vs. N). GMT files for "C2: curated gene sets" and "C5: GO gene sets" were obtained from the MSigDB collections and used separately in the analysis.

Small RNA-sequencing on epithelial cells

To study changes in miRNA expression patterns in the same target cells, we further analyzed the Nitrofen and Nitrofen+rAFSC-EVs treated cells using small RNA-sequencing. Total RNA isolated from n=4 matched samples of Nitrofen and Nitrofen+rAFSC-EVs was used to prepare small RNA libraries (NEBNext small RNA kit) and subjected to miRNA-sequencing. Sequencing libraries were quantified and size selected as described above, and sequenced on a single-end 50-base pair rapid run flowcell. FastQC was used to examine the quality of approximately 1.4 million mapped reads per sample. BBDuk (BBMap suite v37.90) was used to trim adaptor sequences from reads with reference adapter sequences provided by BBMap suite and settings "hdist=1 mink=11" for small RNA-seq reads. For miRNA size specificity, only reads less than 23 nucleotides in length were retained. Following trimming, FastQC was used to examine the quality of trimmed sequenced reads. miRDeep2 (v2.0.0) mapper.pl was used with default parameters to map reads of at least 18 nucleotides in length to rat genome (rnor6). Known and novel miRNAs were identified using miRDeep2 main algorithm (miRDeep2.pl) with default parameters and known mature miRNAs for rat which were obtained from miRBase (v22.1). Only known and novel miRNAs with reported miRDeep score ≥ 2 were retained for downstream analyses.

Counts processing and differential miRNA expression analysis

Prior to differential miRNA expression analysis, read counts were scaled to sample library sizes and read counts per million (CPM) were calculated using R (v3.6.0) edgeR functions "cpm" and "calcNormFactors" (v3.26.5). Only miRNAs with CPM ≥ 1 in at least 3 samples within each condition were retained for downstream analysis. Differentially expressed miRNAs were identified using edgeR. Quasi-likelihood F-test method was used to test for differential expression (FDR < 0.1) for rAFSC-EV-treated and nitrofen-injured lung epithelial cells (NA) compared to nitrofen-injured cells (N).

miRNA-mRNA gene target correlation

Rat orthologs of miRNA-mRNA gene targets were determined from TargetScan (v7.2) and miRTarBase (release v8.0). Only TargetScan gene targets with weighted context score percentile ≥ 50 were retained. Spearman's correlation was calculated using logCPM miRNA expression and logRPKM gene expression for a given pair. miRNA-gene pairs with Spearman's correlation coefficient (rho) < 0 and p-value ≤ 0.05 were considered negatively correlated.

Cargo-seq miRNA-mRNA interaction network

miRNAs with a detected expression value ≥ 2 in rAFSC-EVs were considered in this analysis. miRNA-gene target pairs were determined as outlined above and shown as an interaction network generated using Cytoscape. Target genes that are differentially expressed (FDR < 0.1) and have lower expression in rAFSC-EV-treated samples (log2FC < 0) are shown in the interaction network (blue nodes). miRNAs detected in rAFSC-EVs with higher median logCPM expression in rAFSC-EV-treated and nitrofen-injured primary cells compared to nitrofen-injured untreated cells are considered "miRNA up in primary cells" (green nodes). "miRNA in rAFSC-EV cargo" (white nodes) represent miRNAs detected in rAFSC-EV cargo and are not detected in rAFSC-EV-treated nitrofen-injured primary cells or these miRNAs have lower median logCPM expression in rAFSC-EV-treated nitrofen-injured primary cells compared to nitrofen-injured untreated primary cells.

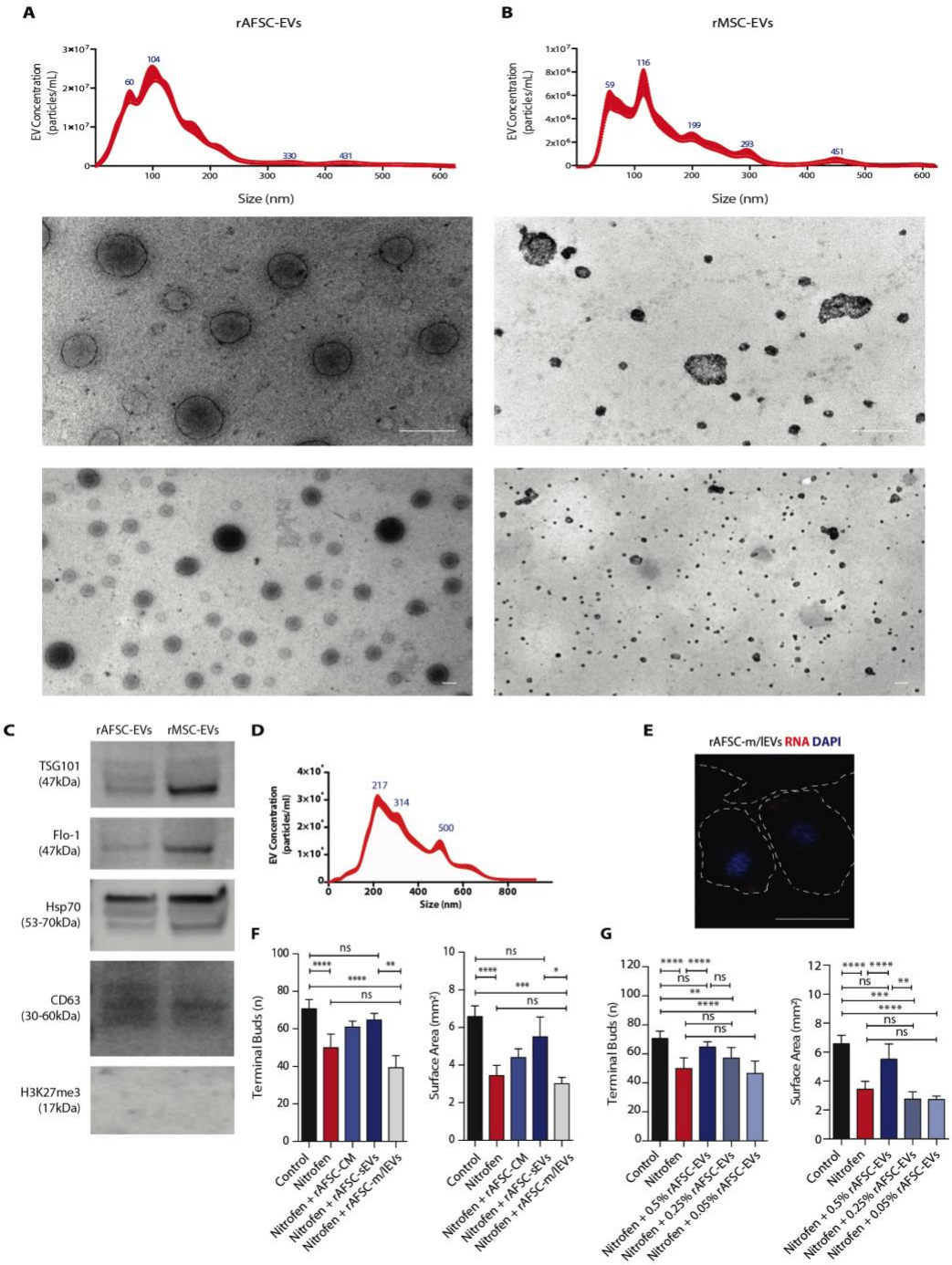

Fig. S1. Characterization of rAFSC-EVs and rMSC-EVs and effects on lung explants based on size and concentration. (**A**) Representative plot of the average size distribution of rAFSC-EVs and rMSC-EVs visualized using nanoparticle tracking analysis. Data are representative of five 40-second videos of each EV preparation. X-axis = size distribution (nm), y-axis = concentration

(particles/mL). (**B**) Representative transmission electron microscopy photos of rAFSC-EVs and rMSC-EVs; two different magnifications highlight the morphology of individual EVs at near fields (top) and far fields (bottom). Scale bar = 200 nm. (**C**) Expression of canonical EV markers TSG101, Flo-1, Hsp70, and CD63 obtained by Western blot analysis for rAFSC-EVs and rMSC-EVs in n=3 technical replicates. EV preparations do not express histone marker H3K27me3. (**D**) Representative plot of the average size distribution of medium/large rAFSC-EVs. Data are representative of five 40-second videos of each EV preparation. X-axis = size distribution (nm), y-axis = concentration (particles/mL). (**E**) Live cell tracking of RNA in medium/large rAFSC-EVs (m/l rAFSC-EVs), DAPI, blue. Scale bar = 100 μm. Cells were outlined based on light microscopy images to highlight the cell border. (**F**) Effects of EV size (small EVs, rAFSC-sEVs; medium/large, m/l rAFSC-EVs) on lung explant terminal bud count and mean surface area in Control (n=16), Nitrofen (n=17), Nitrofen+rAFSC-CM (n=12), Nitrofen+rAFSC-sEVs (n=12), and Nitrofen+rAFSC-m/lEVs (n=4). (**G**) Effects of decreasing doses of rAFSC-EVs (0.5%, 0.25%, 0.05% v/v) on lung explant terminal bud count and mean surface area in Control (n=16), Nitrofen (n=17), Nitrofen+0.5% v/v rAFSC-EVs (n=12), Nitrofen+0.25% v/v rAFSC-EVs (n=5), Nitrofen+0.05% v/v rAFSC-EVs (n=5). Groups were compared using Kruskal-Wallis (post-hoc Dunn's nonparametric comparison) test for fig. S1 F and G, according to Gaussian distribution assessed by D'Agostino Pearson omnibus normality test.

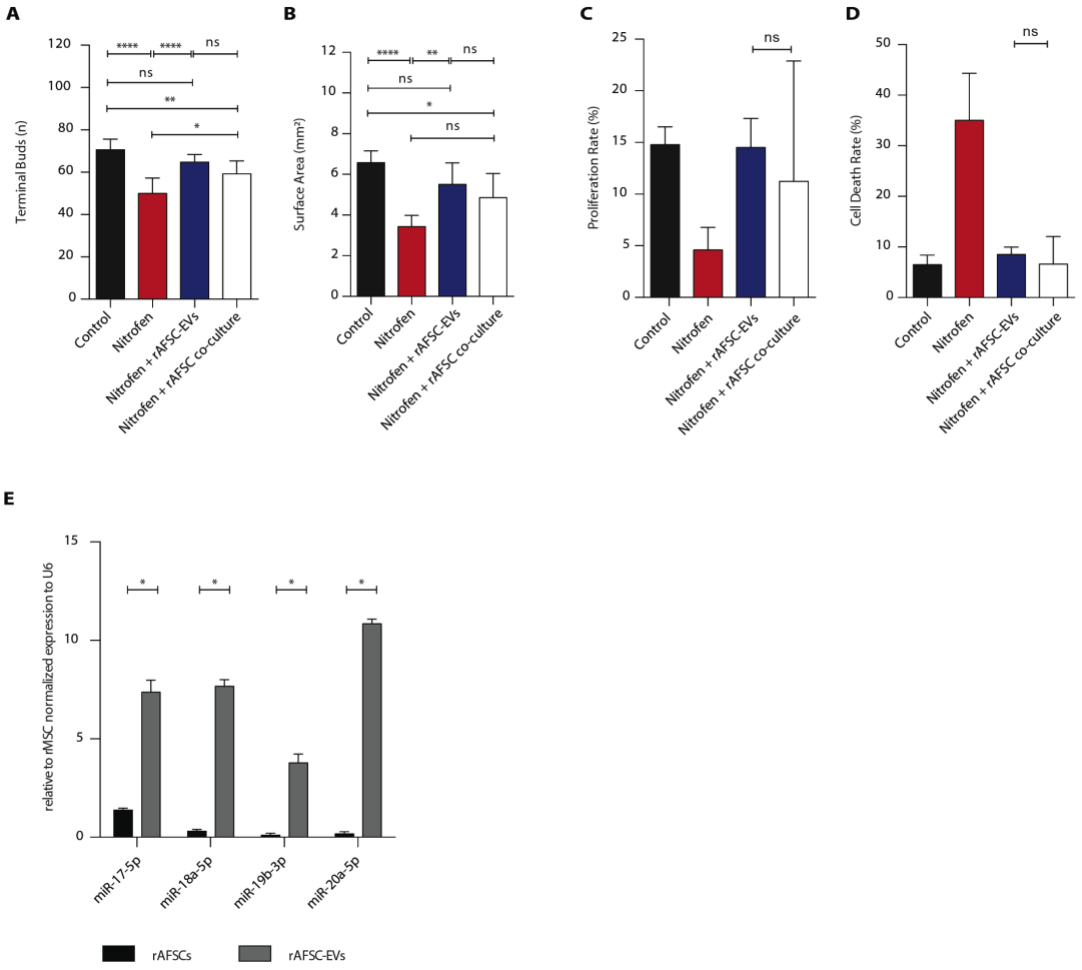

Fig. S2. Influence of rAFSCs in co-culture with ex vivo and in vitro models of pulmonary hypoplasia and effects on rAFSC-EV miRNA cargo. (**A** and **B**) Effects on terminal bud count (A) and mean surface area (B) of nitrofen-injured fetal lung explants co-cultured with rAFSCs at 72 h (n=7 biological replicates). (**C** and **D**) Proliferation rate (**C**) and cell death rate (**D**) of primary lung epithelial cells treated in co-culture with rAFSCs in transwells for 24 h (n=3 biological replicates). (**E**) miRNA expression of rAFSCs compared with rAFSC-EVs through miRCURY LNA SYBR qPCR. Data are shown as normalized relative expression to rMSCs and rMSC-EVs for four members of the miR17~92 family (n=3 matched replicates per each condition). Groups were compared using Kruskal-Wallis (post-hoc Dunn's nonparametric comparison) test for fig. S2

A and B, and with Mann-Whitney test for fig. S2 C and D, according to Gaussian distribution assessed by D'Agostino Pearson omnibus normality test. Groups in fig. S2 E were compared using Holm-Sidak method with alpha=5%, each target was analyzed individually, without assuming a consistent SD.

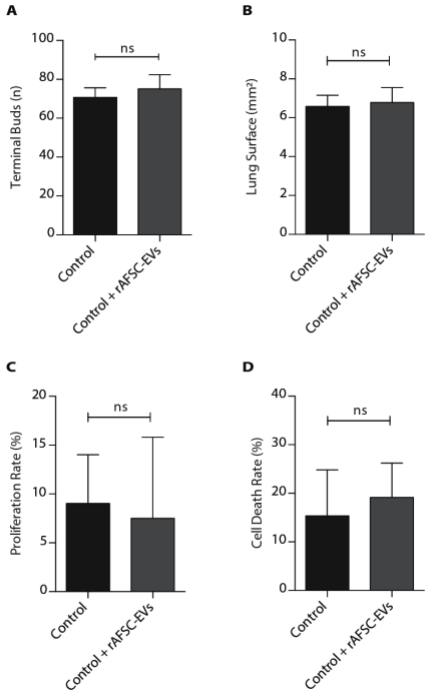

Fig. S3. Effects of rAFSC-EVs on control lung explants and primary lung epithelial cells. (**A** and **B**) Addition of rAFSC-EVs on control lung explants quantified for terminal bud count, (**A**) and lung surface area, (**B**), in Control (n=16) and Control+rAFSC-EVs (n=4). Effects on control primary lung epithelial cells proliferation (**C**), and cell death rates (**D**) in Control (n=4) and Control+rAFSC-EVs (n=3), ns = P>0.05. Groups were compared using Mann-Whitney test for fig. S3 A-D, according to Gaussian distribution assessed by D'Agostino Pearson omnibus normality test.

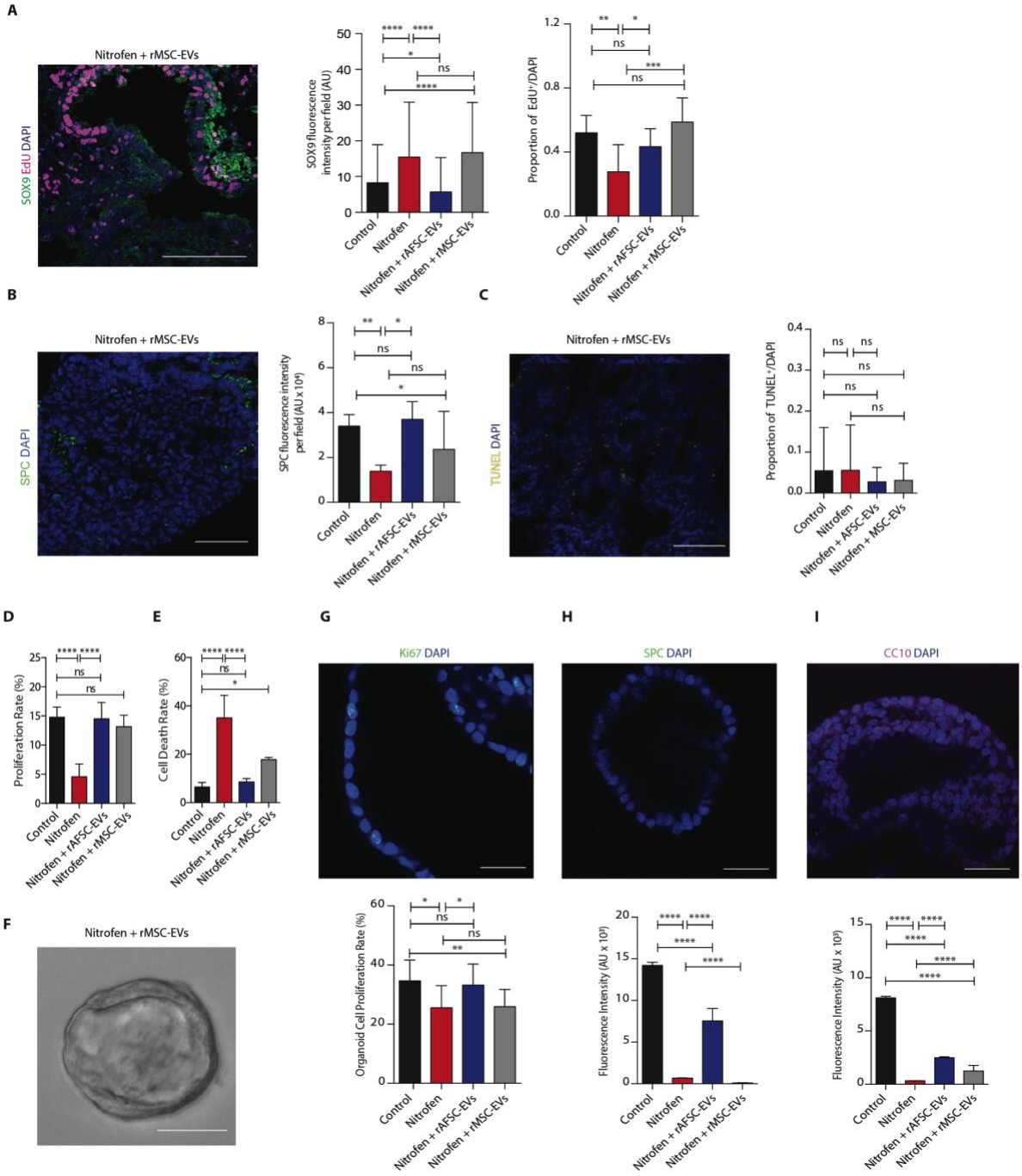

Fig. S4. **Effects of rMSC-EV administration on in vitro and ex vivo models of pulmonary hypoplasia.** (**A**) Immunofluorescence co-stain experiment of proliferating cells and distal lung epithelium progenitor cells of lung explants (SOX9, green; EdU, pink, DAPI nuclear stain, blue;

scale bar = 100 µm), quantified through number of EdU^+ cell per DAPI and SOX9 fluorescence intensity (AU = arbitrary units) in n=4 biological replicates with a total of 50x50 µm fields covering entire lung sections as indicated: Control (n=157), Nitrofen (n=222), Nitrofen+rAFSC-EVs (n=128), Nitrofen+rMSC-EVs (n=122). (**B**) Immunofluorescence experiment of surfactant protein C (SPC) expressing cells in lung explants (SPC, green; DAPI nuclear stain, blue; scale bar=100 µm), quantified by fluorescence intensity: Control (n=6), Nitrofen (n=4), Nitrofen+rAFSC-EVs (n=4), Nitrofen+rMSC-EVs (n=4). (**C**) TUNEL immunofluorescence experiments on lung explants grown for 72 h, quantified by $TUNEL^+$ cells per DAPI in n=4 biological replicates with a total of 50x50 µm fields covering entire lung sections as indicated: Control (n=311), Nitrofen (n=240), Nitrofen+rAFSC-EVs (n=107), Nitrofen+rMSC-EVs (n=191). (**D**) Proliferation rate of primary lung epithelial cells from control and nitrofen-injured hypoplastic lungs treated with medium only, rAFSC-EVs, or rMSC-EVs [5'EdU labeling Control (n=7), Nitrofen (n=5), Nitrofen+rAFSC-EVs (n=5), Nitrofen+rMSC-EVs (n=4)]. (**E**) Cell death rate of primary lung epithelial cells from control and nitrofen-injured hypoplastic lungs treated as in **(D)** (live/dead cytotoxicity assay in Control n=5, Nitrofen (n=5), Nitrofen+rAFSC-EVs (n=5), Nitrofen+rMSC-EVs (n=4). **(F)** Light microscopy photos of fetal rat lung organoids derived from nitrofen-injured hypoplastic lungs treated with rMSC-EVs. Scale bar = 100 µm. Representative photo of n=104 organoids imaged. (**G**) Proliferation of cells in organoids evaluated with immunofluorescence (Ki67 staining, green; scale bar = 50 µm) and quantified as percentage of $Ki67^+$ cells per total number of DAPI (blue) stained nuclei in Control (n=8), Nitrofen (n=7), Nitrofen+rAFSC-EVs (n=9), Nitrofen+rMSC-EVs (n=14). (**H**) SPC staining in organoids (green; DAPI nuclear stain, blue; scale bar = 50 µm) quantified with fluorescence intensity calculated from total corrected cellular fluorescence in Control (n=30), Nitrofen (n=31), Nitrofen+rAFSC-EVs

(n=25), Nitrofen+rMSC-EVs (n=5). (**I**) $CC10^+$ cells in organoids (green; DAPI nuclear stain, blue; scale bar = 50 μm) quantified with fluorescence intensity calculated from total corrected cellular fluorescence in Control (n=30), Nitrofen (n=30), Nitrofen+rAFSC-EVs (n=30), Nitrofen+rMSC-EVs (n=25). Groups were compared using Kruskal-Wallis (post-hoc Dunn's nonparametric comparison) test for fig. S4 A-E, G-I, according to Gaussian distribution assessed by D'Agostino Pearson omnibus normality test.

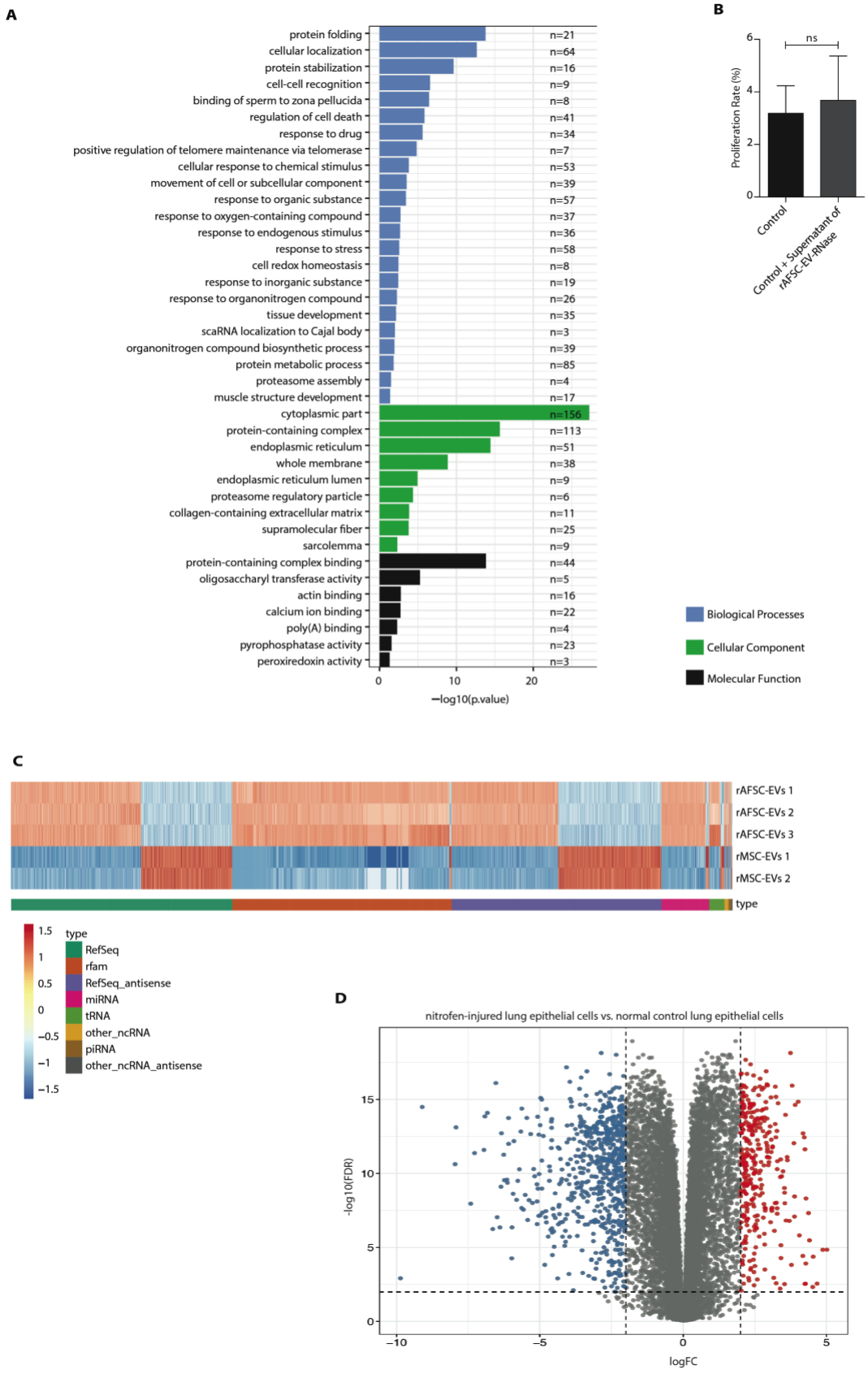
A
protein folding n=21
cellular localization n=64
protein stabilization n=16
cell-cell recognition n=9
binding of sperm to zona pellucida n=8
regulation of cell death n=41
response to drug n=34
positive regulation of telomere maintenance via telomerase n=7
cellular response to chemical stimulus n=53
movement of cell or subcellular component n=39
response to organic substance n=57
response to oxygen-containing compound n=37
response to endogenous stimulus n=36
response to stress n=58
cell redox homeostasis n=8
response to inorganic substance n=19
response to organonitrogen compound n=26
tissue development n=35
scaRNA localization to Cajal body n=3
organonitrogen compound biosynthetic process n=39
protein metabolic process n=85
proteasome assembly n=4
muscle structure development n=17
cytoplasmic part n=156
protein-containing complex n=113
endoplasmic reticulum n=51
whole membrane n=38
endoplasmic reticulum lumen n=9
proteasome regulatory particle n=6
collagen-containing extracellular matrix n=11
supramolecular fiber n=25
sarcolemma n=9
protein-containing complex binding n=44
oligosaccharyl transferase activity n=5
actin binding n=16
calcium ion binding n=22
poly(A) binding n=4
pyrophosphatase activity n=23
peroxiredoxin activity n=3
0
10
20
−log10(p.value)
Biological Processes
Cellular Component
Molecular Function
B
ns
Proliferation Rate (%)
6
4
2
0
Control
Control + Supernatant of rAFSC-EV-RNase
C
rAFSC-EVs 1
rAFSC-EVs 2
rAFSC-EVs 3
rMSC-EVs 1
rMSC-EVs 2
type
1.5
1
0.5
0
−0.5
−1
−1.5
type
RefSeq
rfam
RefSeq_antisense
miRNA
tRNA
other_ncRNA
piRNA
other_ncRNA_antisense
D
nitrofen-injured lung epithelial cells vs. normal control lung epithelial cells
-log10(FDR)
15
10
5
0
−10
−5
0
5
logFC

Fig. S5. Analysis of protein and RNA cargo of rAFSC-EV and rMSC-EV. (A) Pathway enrichment analysis of rAFSC-EV enriched protein cargo in GO terms Biology Processes, Cellular Component, and Molecular Functions. (**B**) Effect of potential carry-over of RNase in rAFSC-EV-RNase experiments on control cell proliferation (n=17 technical replicates). The enzymatically treated rAFSC-EVs were separated from the supernatant, which was then administered to control lung epithelial cells (n=43 technical replicates). Groups were compared using unpaired t-test, according to Gaussian distribution assessed by D'Agostino Pearson omnibus normality test. (**C**) Heatmap showing expression levels of significantly different species of RNA (FDR<0.01) separated by type for cargo from rAFSC-EV (n=3) and rMSC-EV (n=2) samples. Rows and columns are displayed using hierarchical clustering (Ward's method; row distance measure: Pearson correlation; column distance measure: Euclidean). Color scale represents rows scaled (scaled across samples for each gene), log2 transformed normalized counts. (**D**) Volcano plot of genes differentially expressed between nitrofen-injured lung epithelial cells and control (non-nitrofen exposed) lung epithelial cells. Each dot represents a gene with log2 fold change <-2 (lower expression in Nitrofen vs. Control, n=322 red nodes) or >2 (higher expression in Nitrofen vs. Control, n=661 blue nodes).

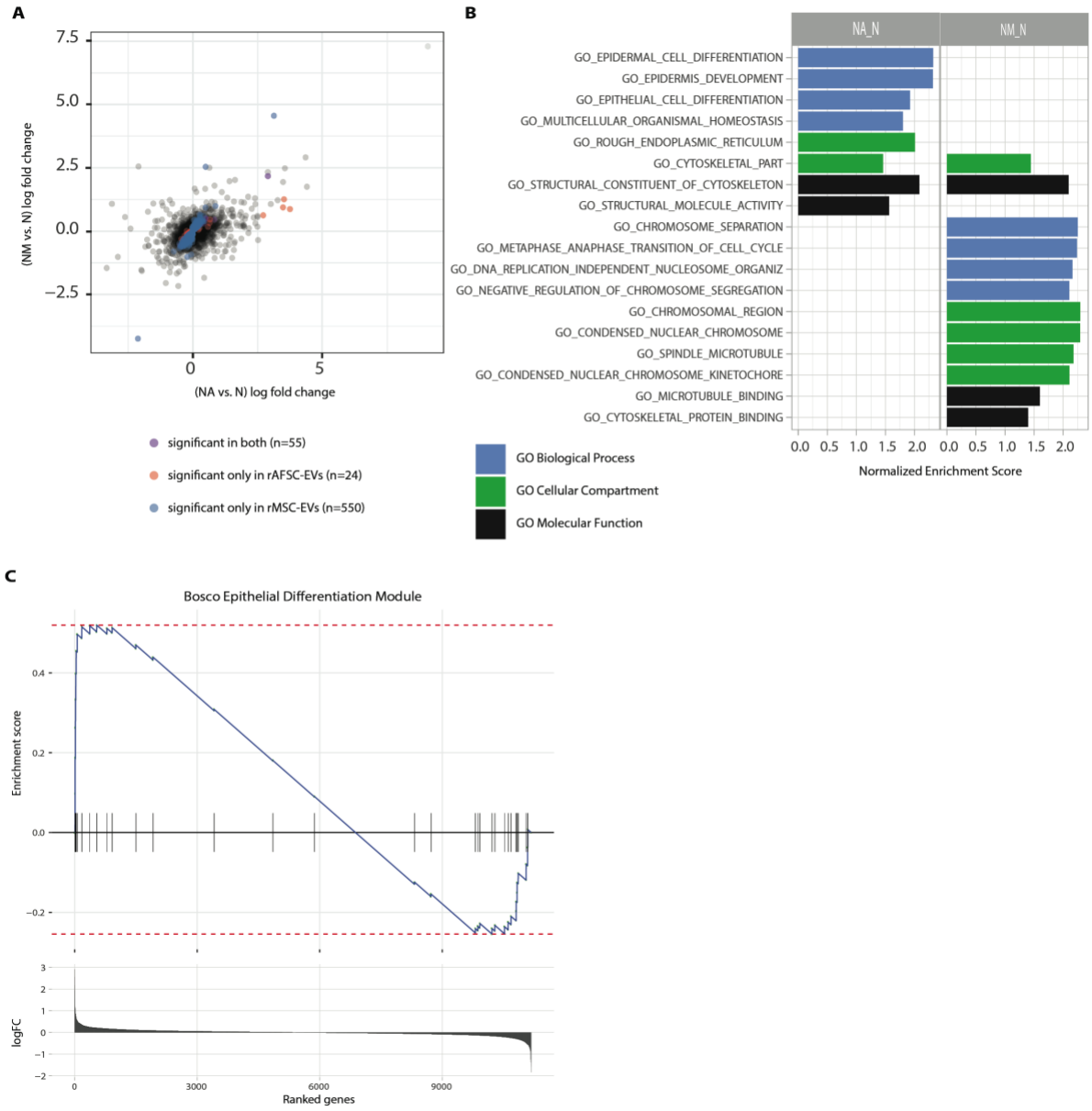

Fig. S6. Enrichment plots for RNA-seq analysis of rMSC-EV treated primary lung epithelial cells. (**A**) Scatterplot of log fold changes between Nitrofen+rAFSC-EVs (NA) vs. Nitrofen (N) and Nitrofen+rMSC-EVs (NM) vs. N. Pearson correlation = 0.54 ($p < 2.2e\text{-}16$, 95% CI [0.53, 0.55]). Each dot represents a gene with its log fold change between NA vs. N shown on the X-axis and log fold change between NM vs. N shown on the Y-axis. Dots are colored based on if the gene is identified as significantly differentially expressed (FDR < 0.1) only in NA vs. N (red), in NM

vs. N (blue), or in both comparisons (purple). See supplementary data file S3 for the full lists of differentially expressed genes. (**B**) Selected pathways identified with gene set enrichment analysis of NA vs. N and NM vs. N primary lung epithelial cells for GO pathways Biological Process, Cellular Component, and Molecular Function. See supplementary data file S4 for full lists of GSEA results. (**C**) GSEA enrichment plot of epithelial cell differentiation generated with all genes ranked by fold changes between Nitrofen vs. Nitrofen+rMSC-EV-treated.

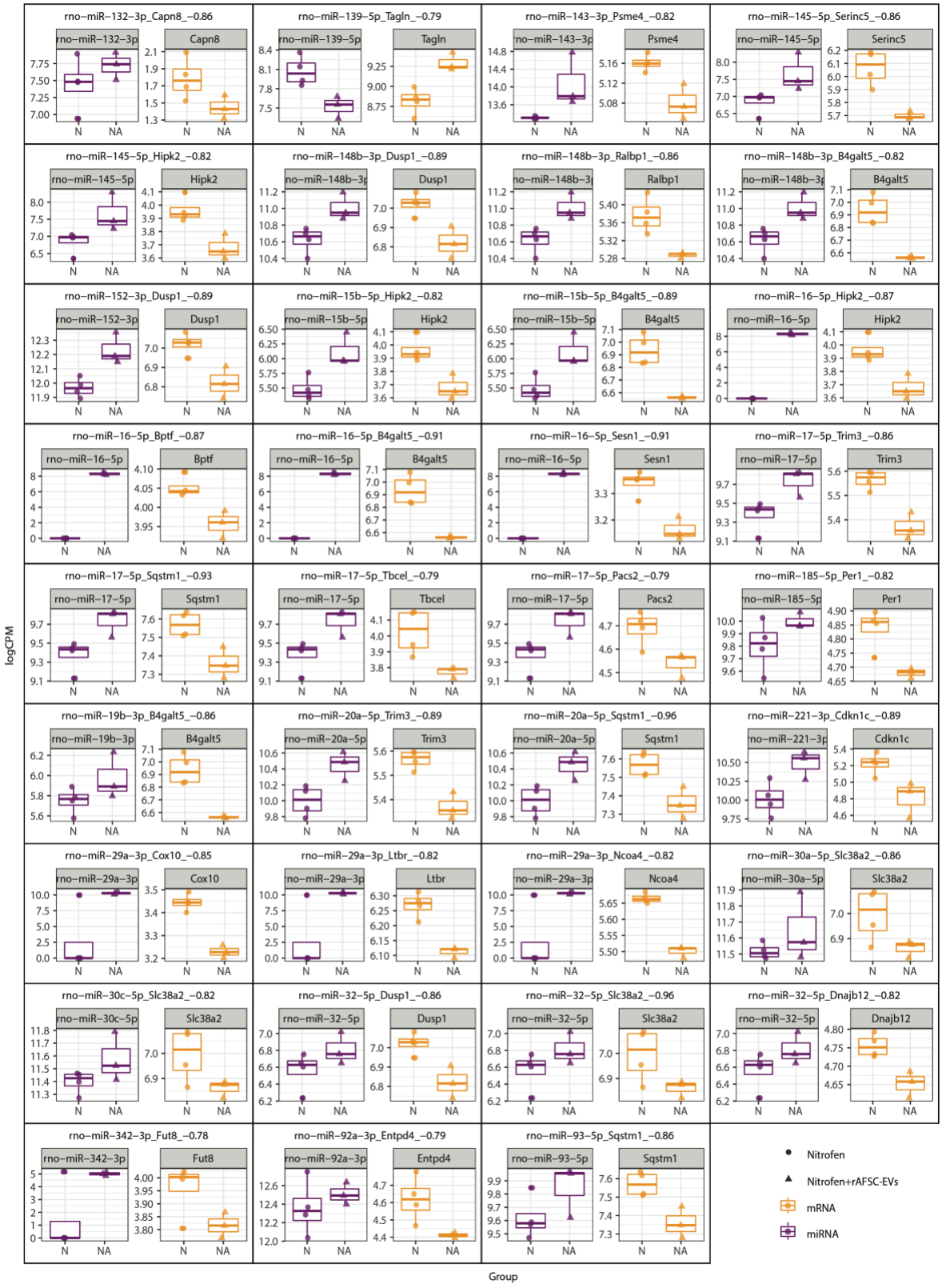

Fig. S7. Correlation analysis of miRNA-mRNA sequencing in primary lung epithelial cells.

Negatively correlated miRNA-mRNA pairs in primary lung epithelial cells are graphed by log of counts per million mapped reads (CPM) of miRNA (purple) and mRNA (orange) for primary lung epithelial cells from Nitrofen (N) and Nitrofen+rAFSC-EVs (NA) conditions. For a given negatively correlated pair (n=3-4 replicates), logCPM expression is shown for miRNA (purple) and gene (orange). Expression is shown for nitrofen-injured lung epithelial cells (Nitrofen, N, circles) and rAFSC-EV-treated nitrofen-injured epithelial cells (Nitrofen+rAFSC-EVs, NA, triangles). Spearman's correlation coefficient (rho) is shown next to the miRNA-mRNA pair label.

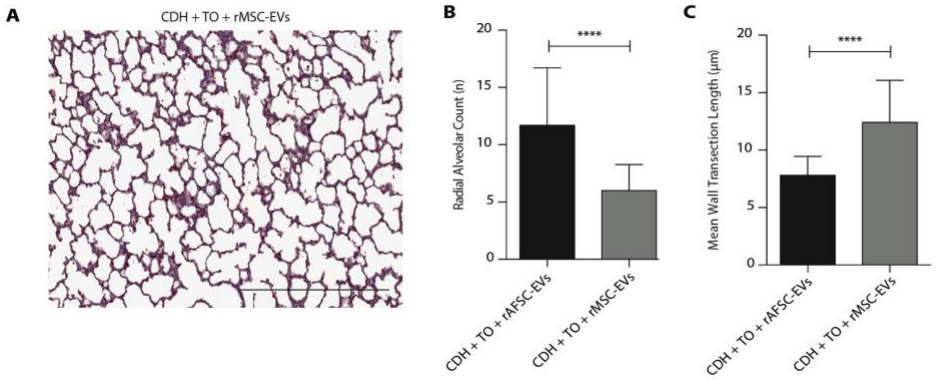

Fig. S8 Effects of rMSC-EV administration in the in vivo model of pulmonary hypoplasia. (**A**) Representative histology images (hematoxylin/eosin) of fetal lungs from fetal rabbits that underwent surgical CDH creation and were subjected to administration of rMSC-EVs prior to tracheal occlusion (CDH+TO+rMSC-EVs). Scale bar = 500 µm. (**B** and **C**) Differences in number of alveoli (radial alveolar count, **B**) and thickness of the alveolar wall (mean wall transection length, **C**) between CDH+TO+rAFSC-EVs (n=9) and CDH+TO+rMSC-EVs (n=8). Groups were compared using Mann-Whitney test for fig. S8 B and C, according to Gaussian distribution assessed by D'Agostino Pearson omnibus normality test.

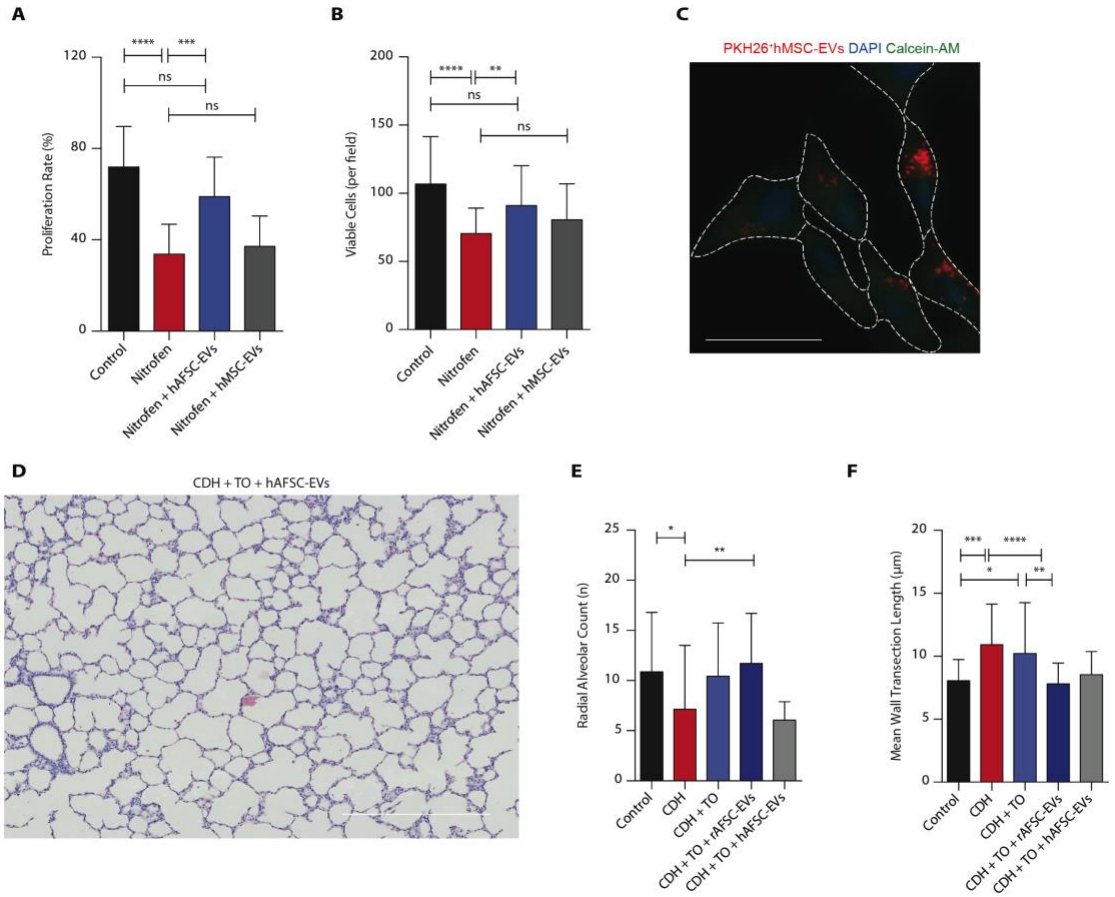

Fig. S9. Effects of hAFSC-EVs and hMSC-EVs on human fetal lung epithelial cells and in the in vivo model of pulmonary hypoplasia. (**A**) Proliferation rate of primary human pulmonary alveolar epithelial cells (HPAEpiC) from a fetus at 21 weeks of gestation, injured with 400 µM of nitrofen exposure for 24 h, and then treated with medium only, or medium supplemented with 0.5% v/v GMP-grade hAFSC-EVs or hMSC-EVs. Replicates were conducted in n=4 technical replicates. (**B**) Number of viable cells per field for the same conditions as in (**A**). (**C**) hMSC-EVs labeled with PKH26 (red signal) entering HPAEpiC (live cells labeled with Calcein-AM, green, nucleus labeled with DAPI, blue). Scale bar = 25 µm. (**D**) Representative histology image (hematoxylin/eosin) of fetal lungs of rabbits that underwent surgical CDH creation and were administered hAFSC-EVs prior to tracheal occlusion (CDH+TO+hAFSC-EVs). Scale bar = 500

μm. Samples are representative of Control (n=9), CDH (n=9), CDH+TO (n=9), CDH+TO+rAFSC-EVs (n=9), and CDH+TO+hAFSC-EVs (n=5). (**E** and **F**) Differences in number of alveoli (radial alveolar count, **E**) and thickness of the alveolar wall (mean wall transection length, **F**). Groups were compared using Kruskal-Wallis (post-hoc Dunn's nonparametric comparison) test for fig. S9 A, B, E, and F, according to Gaussian distribution assessed by D'Agostino Pearson omnibus normality test.

Table S1: Highlighted proteins expressed in rAFSC-EVs and rMSC-EVs.

Identified proteins	**Molecular weight (kDa)**	**Average NSAF rMSC**	**Average NSAF rAFSC**	**p-value for fold change rAFSC / rMSC**
Anxa1	39	0.000	0.017	0.000
Anxa11	54	0.000	0.001	0.122
Anxa2	39	0.012	0.019	0.232
Anxa3	36	0.000	0.001	0.374
Anxa4	36	0.000	0.003	0.011
Anxa5	36	0.000	0.012	0.000
Anxa6	76	0.000	0.012	0.000
Anxa7	50	0.000	0.002	0.000
Cd63	26	0.000	0.001	0.001
Celf1	52	0.000	0.000	0.374
Hnrnpa1	34	0.000	0.001	0.157
Hnrnpa2b1	32	0.000	0.001	0.118
Hnrnpc	33	0.000	0.000	0.374
Hnrnpf	46	0.000	0.001	0.001
Hnrnph1	49	0.000	0.002	0.000
Hnrnpk	51	0.000	0.001	0.028
Hnrnpl	68	0.000	0.001	0.165
Hnrnpm	74	0.000	0.001	0.036
Hnrnpu	88	0.000	0.002	0.017
Hnrnpul2	85	0.000	0.000	0.001
Hspa1a	70	0.000	0.003	0.000
Hspa2	70	0.000	0.001	0.374
Hspa4	94	0.000	0.000	0.374
Hspa5	72	0.008	0.010	0.032
Hspa8	71	0.011	0.012	0.575
Hspa9	74	0.000	0.002	0.000

kDa: kilodaltons
NSAF: normalized spectral abundance factor
rAFSCs: rat amniotic fluid stem cells
rMSCs: rat mesenchymal stromal cells

Table S2: miRNAs related to lung development that are differentially expressed in rAFSC-EVs over rMSC-EVs.

miRNA	miR ID	chr	start	end	type	rMSCs	rAFSCs	log_2Fold Change	adjusted p-value	Relevance
miR-17	rno-miR-17-5p	chr15	103640915	103640937	+	59.87	22473.82	8.5522	0	The mir 17-92 cluster and its paralogues:
	rno-mir-17-2	chrX	140167738	140167815	-	59.87	22473.82	8.5522	0	
	rno-mir-17-1	chr15	103640902	103640985	+	65.28	22863.5	8.4522	0	
	rno-miR-17-1-3p	chr15	103640952	103640973	+	0.71	177.19	7.958	0	
miR-18	rno-miR-18a-5p	chr15	103641054	103641076	+	3.07	953.84	8.2779	0	- control FGF10-mediated embryonic lung epithelial branching morphogenesis (*69*);
	rno-mir-18a	chr15	103641038	103641133	+	5.28	1034.37	7.6146	0	
	rno-miR-18a-3p	chr15	103641095	103641115	+	2.2	81.58	5.2098	0	
miR-19	rno-miR-19a-5p	chr15	103641197	103641216	+	0	1.08	Inf	1	- control lung progenitor cell proliferation and differentiation (*59, 69*);
	rno-miR-19b-1-5p	chr15	103641502	103641523	+	0	1.05	Inf	1	
	rno-mir-19a	chr15	103641185	103641266	+	2.71	1007.59	8.5407	0	
	rno-miR-19a-3p	chr15	103641233	103641255	+	2.71	1006.52	8.5392	0	
	rno-mir-19b-2	chrX	140167226	140167321	-	16.7	5235.41	8.2922	0	
	rno-miR-19b-3p	chr15	103641540	103641562	+	16.7	5235.41	8.2922	0	
	rno-mir-19b-1	chr15	103641487	103641573	+	16.7	5231.7	8.2912	0	
miR-20	rno-miR-20a-3p	chr15	103641408	103641428	+	0	1.6	Inf	0.8997	- regulate embryonic growth, apoptosis, and fetal lung development (*9*);
	rno-miR-20a-5p	chr15	103641372	103641394	+	30.04	19844.96	9.3677	0	
	rno-mir-20a	chr15	103641357	103641441	+	30.04	19844.96	9.3677	0	
	rno-miR-20b-5p	chrX	140167407	140167429	-	0.51	21.61	5.3986	0.0038	
	rno-mir-20b	chrX	140167365	140167436	-	0.51	21.61	5.3986	0.0038	
miR-92	rno-miR-92b-5p	chr2	207955729	207955752	-	0.2	1.62	3.0149	1	- regulate surfactant protein C secretion (miR19b and 92a) (*70*);
	rno-miR-92a-1-5p	chr15	103641619	103641641	+	2.2	15.58	2.8214	0.1041	
	rno-mir-92a-1	chr15	103641609	103641686	+	1466.75	3152.85	1.104	0.0346	
	rno-miR-92a-3p	chr15	103641656	103641676	+	447.53	519.1	0.214	1	
	rno-mir-92a-2	chrX	140167096	140167187	-	447.53	519.1	0.214	1	
	rno-mir-92b	chr2	207955680	207955762	-	404.68	109.76	-1.8824	0.1754	
	rno-miR-92b-3p	chr2	207955690	207955711	-	404.48	108.14	-1.9032	0.1696	
miR-106	rno-miR-106b-5p	chr12	21365432	21365452	-	12.55	2451.88	7.6103	0	- are involved in alveolarization processes (mir17) (*71*).
	rno-mir-106b	chr12	21365382	21365463	-	302.19	12390.58	5.3576	0	
	rno-miR-106b-3p	chr12	21365391	21365412	-	289.64	9939.25	5.1008	0	
miR-363	rno-miR-363-3p	chrX	140166956	140166976	-	3.21	3.72	0.2128	1	
	rno-mir-363	chrX	140166945	140167031	-	4.49	3.72	-0.2719	1	

miR-93	rno-miR-93-5p	chr12	21365223	21365245	-	953.63	108642.09	6.8319	0	
	rno-mir-93	chr12	21365173	21365259	-	955.42	108717.23	6.8302	0	
	rno-miR-93-3p	chr12	21365185	21365207	-	1.79	75.15	5.3896	0	
miR-25	rno-miR-25-3p	chr12	21364981	21365002	-	5238.63	83820.36	4	0	
	rno-mir-25	chr12	21364970	21365053	-	5262.06	83911.87	3.9952	0	
	rno-miR-25-5p	chr12	21365019	21365040	-	23.43	90.98	1.9574	0.0033	
miR-7	rno-miR-7b	chr9	9803964	9803986	-	0	66.56	Inf	0	- miRNAs involved in surfactant protein C secretion and expressed in human ATI and/or ATII cells (*70*).
	rno-mir-7b	chr9	9803905	9804014	-	0	66.56	Inf	0	
	rno-miR-7a-2-3p	chr1	141551398	141551419	+	0	2.68	Inf	0.6528	
	rno-mir-7a-2	chr1	141551342	141551436	+	111.49	133696.6	10.2279	0	
	rno-miR-7a-5p	chr1	141551360	141551382	+	119.28	133897.01	10.1325	0	
	rno-mir-7a-1	chr17	8879389	8879485	+	125.25	133996	10.0632	0	
	rno-miR-7a-1-3p	chr17	8879448	8879469	+	5.97	97.89	4.0358	0	
let7-f-1 and let7-f-2	rno-let-7f-1-3p	chr17	18474397	18474417	+	0	37.3	Inf	4.00E-04	
	rno-let-7f-1	chr17	18474334	18474422	+	6660.85	188375.58	4.8218	0	
	rno-let-7f-5p	chr17	18474341	18474362	+	7068.36	189106.28	4.7417	0	
	rno-let-7f-2	chrX	21868509	21868591	-	7072.71	189158.31	4.7412	0	
	rno-let-7f-2-3p	chrX	21868514	21868534	-	3.59	42.95	3.5827	0	
rno-mir-219a-1	rno-mir-219a-1	chr20	5895489	5895598	-	10.69	85.29	2.9963	0	
	rno-miR-219a-1-3p	chr20	5895516	5895537	-	10.69	83.16	2.9598	0	
miR-103	rno-mir-103-2	chr3	130329252	130329337	+	3229.37	40889.34	3.6624	0	
	rno-miR-103-3p	chr10	20480402	20480424	+	3229.37	40883.42	3.6622	0	
	rno-mir-103-1	chr10	20480351	20480436	+	3234.27	40892.4	3.6603	0	
miR-125b-1	rno-miR-125b-1-3p	chr8	44272900	44272921	+	7472.2	19346.02	1.3724	0.002	

						7718.5				
	rno-mir-125b-1	chr8	44272846	44272932	+	9	19862	1.3636	0.0022	
mir-129-1	rno-miR-129-1-3p	chr4	56049143	56049161	+	0	2.66	Inf	0.5709	
	rno-mir-129-1	chr4	56049095	56049166	+	369.44	5715.96	3.9516	0	
miR-542	rno-miR-542-3p	chrX	152777501	152777522	+	47.45	14042.5	8.2091	0	
	rno-mir-542-1	chrX	152777453	152777531	+	60.06	14313.6	7.8968	0	
	rno-mir-542-2	chrX	152784192	152784270	+	60.06	14313.6	7.8968	0	
	rno-mir-542-3	chrX	153215172	153215250	+	60.06	14313.6	7.8968	0	
	rno-miR-542-5p	chrX	152777463	152777484	+	12.6	265.18	4.395	0	
miR-592	rno-mir-592	chr4	54925353	54925448	-	18.39	4706.09	7.9992	0	
	rno-miR-592	chr4	54925409	54925431	-	18.39	4705.01	7.9989	0	
miR-138	rno-miR-138-5p	chr19	11127530	11127552	-	5.59	109.53	4.2925	0	- miRNAs that regulate late stage murine lung development and are significantly different with sex and gestational age in E15-E18 lungs (*72*).
	rno-mir-138-1	chr8	130886768	130886866	+	5.85	109.53	4.2279	0	
	rno-mir-138-2	chr19	11127479	11127560	-	6.87	124.48	4.1794	0	
	rno-miR-138-2-3p	chr19	11127485	11127505	-	1.28	19.31	3.9144	0.0039	
miR-182	rno-miR-182	chr4	57221577	57221601	-	40.34	994.77	4.6241	0	
	rno-mir-182	chr4	57221574	57221635	-	40.34	994.77	4.6241	0	
mir-296	rno-miR-296-5p	chr3	178408833	178408853	-	0.6	41.26	6.1007	0	
	rno-mir-296	chr3	178408788	178408865	-	116.43	516.99	2.1507	0	
	rno-miR-296-3p	chr3	178408798	178408819	-	115.83	471.97	2.0267	4.00E-04	
miR-471	rno-miR-471-3p	chrX	151267019	151267038	-	0	66.6	Inf	0	- miRNAs involved in alveolarization and significantly changed in P10 or P20 lungs in a model of intrauterine growth restriction (*71*).
	rno-mir-471	chrX	151267006	151267083	-	0.71	691.21	9.9218	0	
	rno-miR-471-5p	chrX	151267052	151267073	-	0.71	621.36	9.7681	0	
miR-455	rno-miR-455-5p	chr5	83211466	83211487	+	120.43	1324.53	3.4593	0	
miR-322	rno-miR-322-3p	chrX	152773528	152773547	+	62.07	6528.84	6.7167	0	
	rno-miR-322-5p	chrX	152773490	152773511	+	11.56	2847.63	7.9448	0	
	rno-mir-322-1	chrX	152773468	152773562	+	73.63	9392	6.995	0	
	rno-mir-322-2	chrX	153211185	153211279	+	73.63	9392	6.995	0	
	rno-miR-322-3p	chrX	152773528	152773547	+	62.07	6528.84	6.7167	0	
miR-183	rno-mir-183	chr4	57225370	57225479	-	13.24	316.45	4.5792	0	
	rno-miR-183-5p	chr4	57225432	57225453	-	13.24	315.9	4.5767	0	
miR-214	rno-miR-214-5p	chr13	85024828	85024844	+	50.79	1468.47	4.8535	0	
miR-130	rno-miR-130a-5p	chr3	78661749	78661770	-	0	10.72	Inf	0.0051	

	rno-miR-130b-3p	chr11	91182370	91182391	+	251.24	18538.82	6.2053	0	
	rno-mir-130b	chr11	91182320	91182401	+	254.57	18584.85	6.1899	0	
	rno-mir-130a	chr3	78661697	78661784	-	1092.4 8	20003.91	4.1946	0	
	rno-miR-130a-3p	chr3	78661709	78661730	-	1092.4 8	19991.05	4.1937	0	
	rno-miR-130b-5p	chr11	91182332	91182353	+	3.33	44.39	3.7371	0.09	
miR-463	rno-miR-463-3p	chrX	151270941	151270962	-	0	2165.36	Inf	0	- miRNAs involved in the regulation of pluripotency and the reprogramming process in rats (*73*).
	rno-mir-463	chrX	151270931	151271008	-	0.26	3748.68	13.8374	0	
	rno-miR-463-5p	chrX	151270979	151270999	-	0.26	1582.78	12.5935	0	
miR-465	rno-mir-465	chrX	151292178	151292254	-	0	2167.1	Inf	0	
	rno-miR-465-5p	chrX	151292223	151292244	-	0	2096.67	Inf	0	
	rno-miR-465-3p	chrX	151292189	151292210	-	0	68.81	Inf	0	
miR-471	rno-miR-471-3p	chrX	151267019	151267038	-	0	66.6	Inf	0	
	rno-mir-471	chrX	151267006	151267083	-	0.71	691.21	9.9218	0	
	rno-miR-471-5p	chrX	151267052	151267073	-	0.71	621.36	9.7681	0	
miR-741	rno-miR-741-3p	chrX	151269275	151269296	-	0	816.46	Inf	0	
	rno-mir-741	chrX	151269258	151269353	-	0	816.46	Inf	0	
miR-743b	rno-mir-743b	chrX	151248558	151248634	-	0	3809.35	Inf	0	
	rno-miR-743b-5p	chrX	151248603	151248624	-	0	2753.09	Inf	0	
	rno-miR-743b-3p	chrX	151248568	151248589	-	0	1054.16	Inf	0	
miR-871	rno-mir-871	chrX	151282689	151282765	-	0	7147.82	Inf	0	
	rno-miR-871-5p	chrX	151282732	151282755	-	0	7109.67	Inf	0	
	rno-miR-871-3p	chrX	151282700	151282721	-	0	38.15	Inf	0	
miR-881	rno-mir-881	chrX	151278812	151278888	-	0	2210.79	Inf	0	
	rno-miR-881-3p	chrX	151278823	151278844	-	0	1995.88	Inf	0	
	rno-miR-881-5p	chrX	151278860	151278878	-	0	214.9	Inf	0	
miR-883	rno-mir-883	chrX	151255943	151256019	-	0	185.76	Inf	0	
	rno-miR-883-3p	chrX	151255953	151255974	-	0	175.6	Inf	0	
	rno-miR-883-5p	chrX	151255988	151256010	-	0	10.16	Inf	0.0072	
miR-3580	rno-mir-3580	chrX	151290426	151290506	-	0	4306.44	Inf	0	
	rno-miR-3580-3p	chrX	151290438	151290459	-	0	4168.11	Inf	0	
	rno-miR-3580-5p	chrX	151290472	151290493	-	0	138.34	Inf	0	

miR: miRNA; rAFSCs: rat amniotic fluid stem cells; rMSCs: rat mesenchymal stem cells; chr: chromosome; inf: infinity; ATI: alveolar type I cells; ATII: alveolar type II cells.

Table S3: miRNAs known to be involved in pulmonary hypoplasia and present in rAFSC-EVs.

miRNA	miR ID	chr	start	end	type	rMSCs	rAFSCs	log_2Fold Change	adjusted p-value	Relevance
miR-200	rno-miR-200a-5p	chr5	176963441	176963461	-	0.51	0	Inf	1	- miRNAs dysregulated in pulmonary hypoplasia secondary to CDH (*12*, *74-76*).
	rno-mir-200b	chr5	176964166	176964260	-	4.65	0	Inf	0.4715	
	rno-miR-200b-3p	chr5	176964182	176964204	-	1.54	0	Inf	1	
	rno-miR-200b-5p	chr5	176964219	176964240	-	3.12	0	Inf	0.7365	
	rno-miR-200c-5p	chr4	224254426	224254446	-	0	0.55	Inf	1	
	rno-mir-200c	chr4	224254382	224254450	-	12.7	65.95	2.376	0.0014	
	rno-miR-200c-3p	chr4	224254386	224254406	-	12.7	65.95	2.376	0.0014	
	rno-miR-200a-3p	chr5	176963402	176963423	-	5.57	3.8	-0.5508	1	
	rno-mir-200a	chr5	176963388	176963476	-	6.08	3.8	-0.6778	1	
miR-10	rno-miR-10b-3p	chr3	68113726	68113746	+	27.86	172.28	2.6286	1.00E-04	
	rno-mir-10b	chr3	68113662	68113770	+	29928.19	88517.54	1.5645	4.00E-04	
	rno-miR-10b-5p	chr3	68113689	68113710	+	29900.33	88350.61	1.5631	4.00E-04	
	rno-miR-10a-3p	chr10	83968744	83968765	+	4.78	2.66	-0.8426	1	
	rno-mir-10a	chr10	83968682	83968791	+	727.64	88.91	-3.0328	0.0256	
	rno-miR-10a-5p	chr10	83968703	83968725	+	722.86	86.25	-3.0671	0.0232	
miR-33	rno-miR-33-3p	chr7	123415348	123415368	+	0	4.83	Inf	0.1942	- miRNAs downregulated in hypoplastic lungs of experimental CDH (nitrofen model) (*10*).
	rno-mir-33	chr7	123415303	123415371	+	3.94	49.49	3.6504	0	
	rno-miR-33-5p	chr7	123415308	123415328	+	2.43	33.88	3.8032	2.00E-04	
miR-193	rno-mir-193b	chr14	30144277	30144359	-	43.73	552.81	3.66	0	
	rno-miR-193b-3p	chr14	30144291	30144309	-	2.88	543.63	7.5585	0	
	rno-miR-193a-3p	chr10	64583983	64584004	-	2.32	22.62	3.2878	0.0117	
	rno-mir-193a	chr10	64583972	64584057	-	60.8	160.84	1.4034	0.0185	
	rno-miR-193a-5p	chr10	64584017	64584038	-	56.55	138.22	1.2894	0.0417	
	rno-miR-193b-5p	chr14	30144328	30144345	-	40.85	6.45	-2.6624	0.1982	
miR-338	rno-mir-338	chr10	108793410	108793475	-	0	16.14	Inf	2.00E-04	
	rno-miR-338-3p	chr10	108793413	108793435	-	0	8.1	Inf	0.0761	
	rno-miR-338-5p	chr10	108793449	108793470	-	0	8.04	Inf	0.0266	
	rno-mir-30a	chr9	28377823	28377893	+	6702.06	91515.55	3.7713	0	
	rno-miR-30a-5p	chr9	28377828	28377849	+	6239.92	88950.46	3.8334	0	

miR-30a and miR-30c	rno-miR-30a-3p	chr9	28377869	28377890	+	462.13	2565.09	2.4726	0
	rno-mir-30c-2	chr9	28397564	28397647	+	126.18	1532.57	3.6024	0
	rno-mir-30c-1	chr5	143494757	143494845	-	113.57	1523.39	3.7457	0
	rno-miR-30c-5p	chr5	143494807	143494829	-	110.28	1483.2	3.7494	0
	rno-miR-30c-1-3p	chr5	143494769	143494790	-	3.28	40.71	3.6316	1.00E-04
	rno-miR-30c-2-3p	chr9	28397617	28397638	+	15.9	49.37	1.6346	0.0871
miR-22	rno-miR-22-3p	chr10	62013698	62013719	+	11519.53	80600.86	2.8067	0
	rno-miR-22-5p	chr10	62013660	62013681	+	43.31	499.36	3.5272	0
	rno-mir-22	chr10	62013642	62013736	+	11562.84	81100.22	2.8102	0
miR-532	rno-mir-532	chrX	16894994	16895072	+	9.75	128.96	3.7249	0
	rno-miR-532-5p	chrX	16895004	16895025	+	3.92	94.01	4.5842	0
	rno-miR-532-3p	chrX	16895041	16895062	+	5.83	34.95	2.5827	0.013
miR-28	rno-miR-28-3p	chr11	81345228	81345249	+	1115.34	34443.35	4.9487	0
	rno-miR-28-5p	chr11	81345188	81345209	+	76.11	3651.38	5.5842	0
	rno-mir-28	chr11	81345175	81345260	+	1191.45	38095.82	4.9988	0
miR-362	rno-mir-362	chrX	16902294	16902358	+	0	115.82	Inf	0
	rno-miR-362-3p	chrX	16902335	16902356	+	0	114.72	Inf	0
	rno-miR-362-5p	chrX	16902298	16902321	+	0	1.09	Inf	1
miR-3559	rno-mir-3559	chrX	76261608	76261722	-	26.31	1132.64	5.4279	0
	rno-miR-3559-3p	chrX	76261633	76261654	-	21.44	712.18	5.0536	0
	rno-miR-3559-5p	chrX	76261673	76261694	-	4.87	420.45	6.4331	0

miR: miRNA; rAFSCs: rat amniotic fluid stem cells; rMSCs: rat mesenchymal stem cells; chr: chromosome; inf: infinity.

Table S4: Genes differentially expressed in nitrofen-injured lung epithelial cells

Gene	Name	Link to lung development or epithelial homeostasis	Ref.
Down-regulated			
Nkx2.1	NK2 Homeobox 1	Essential regulator of lung development and a marker of early lung epithelial progenitor	(*77*)
Hipk2	Homeodomain Interacting Protein Kinase 2	NKX2-1 binding partner	(*78*)
Alcam	Activated Leukocyte Cell Adhesion Molecule	Marker of type II alveolar epithelial cells	(*79*)
Mxd4	MAX Dimerization Protein 4	Highly prioritized gene in neonates with pulmonary hypoplasia /CDH	(*80*)
Arg2	Arginase 2	Overexpressed gene in neonates with pulmonary hypoplasia/CDH	(*81*)
Fgfr3	Fibroblast Growth Factor Receptor 3	Upregulation of FGFR3 disrupts alveologenesis in experimental and human pulmonary hypoplasia/CDH.	(*80, 82*)
Sult1a1	Sulfotransferase Family 1A Member 1	Upregulated in hypoxic lung injury, and required for nitrofen activation and mutagenicity	(*83, 84*)
Dusp1	Dual Specificity Phosphatase 1	Negatively regulates autophagy, a process required for fetal lung branching morphogenesis	(*85, 86*)
Sqstm1	Sequestosome 1	Marker of autophagy impairment increased in stressed conditions	(*86, 87*)
Ncao4	Nuclear Receptor Coactivator 4	Involved in ferritin turnover and autophagy regulation	(*88*)
Herpud1	Homocysteine Inducible ER Protein With Ubiquitin Like Domain 1	Involved in ER stress response, a critical process for tissue homeostasis that is dysregulated in pulmonary hypoplasia	(*40, 89*)

Cdkn1c	Cyclin Dependent Kinase Inhibitor 1C	Highly expressed in pulmonary hypoplasia	(*90*)
Fuca2	Alpha-L-Fucosidase 2	Involved in repair of damaged lung epithelial cells	(*91*)
Clic3	Chloride Intracellular Channel 3	Activator of MAPK signaling, a pathway that is upregulated in nitrofen-injured lung epithelial cells	(*61*, *92*)
Sesn1	Sestrin 1	Repressor of PDGFRβ signaling, a pathway that is dysregulated in nitrofen lungs	(*93*)
Flcn	Folliculin	Involved in EGFR signaling, a pathway that is down-regulated in pulmonary hypoplasia.	(*94*, *95*)
Up-regulated			
Flna	Filamin A	Actin-binding protein involved in ciliogenesis, FLNA mutations are associated with severe diffuse lung disease and alveolar simplification	(*96*, *97*)
Pdlim5	PDZ And LIM Domain 5	Scaffolding protein that is required for TGF-β/Smad signaling in alveolar epithelial cells, and that prevents hypoxia-induced pulmonary hypertension	(*98*)
Gldn	Gliomedin	ECM matrix glycoprotein (up-regulated by TGF-β signaling)	(*99*)
Igf1r	Insulin Like Growth Factor 1 Receptor	Involved in epithelial proliferation and differentiation, (downregulated in nitrofen)	(*32*)
Gnaq	G Protein Subunit Alpha Q	Nucleotide-binding protein expressed in alveolar Type II epithelial cells that controls surfactant homeostasis	(*100*)
Myh9l1	Myosin Heavy Chain 9 non-muscle-like 1	Protein important for epithelial cell tight junction formation	(*101*)
Clic1	Chloride Intracellular Channel 1	Mitochondria and ER chloride channel protein that regulates redox balance and ER stress	(*40*, *102*)

Hikeshi	Heat Shock Protein Nuclear Import Factor Hikeshi	Nuclear transport receptor required for organization and function of the secretory apparatus in club cells	(*103*)
Cxcl2	C-X-C Motif Chemokine Ligand 2	Cytokine that stimulates proliferation in rat alveolar epithelial cells.	(*104*)

Table S5: Inter-species conservation of top enriched miRNA in hAFSC-EVs

Human miRNA	Rabbit miRNA orthologue	Sequence
hsa-let-7b-5p	ocu-let-7b	5`-UGAGGUAGUAGGUUGUGUGGUU-3`
hsa-miR-23a-3p	ocu-miR-23b-3p	5`-AUCACAUUGCCAGGGAUUUCC-3`
hsa-miR-24-3p	ocu-miR-24-3p	5`-UGGCUCAGUUCAGCAGGAACAG-3`
hsa-miR-31-5p	ocu-miR-31-5p	5`-AGGCAAGAUGCUGGCAUAGCU-3`
hsa-miR-92a-3p	ocu-miR-92a-3p	5`-UAUUGCACUUGUCCCGGCCUGU-3`
hsa-miR-100-5p	ocu-miR-100-5p	5`-AACCCGUAGAUCCGAACUUGUG-3`
hsa-miR-103a-3p	ocu-miR-103a-3p	5`-AGCAGCAUUGUACAGGGCUAUGA-3`
hsa-miR-107	ocu-miR-107-3p	5`-AGCAGCAUUGUACAGGGCUAUCA-3`
hsa-miR-221-3p	ocu-miR-221-3p	5`-AGCUACAUUGUCUGCUGGGUUUC-3`
hsa-miR-222-3p	ocu-miR-222-3p	5`-AGCUACAUCUGGCUACUGGGU-3`
hsa-miR-23b-3p	ocu-miR-23b-3p	5`-AUCACAUUGCCAGGGAUUACCAC-3`
hsa-miR-125b-5p	ocu-miR-125b-5p	5`-UCCCUGAGACCCUAACUUGUGA-3`
hsa-miR-145-5p	ocu-miR-145-5p	5`-GUCCAGUUUUCCCAGGAAUCCCU-3`
hsa-miR-320c	ocu-miR-197-3p	5`-AAAAGCUGGGUUGAGAGGGU-3`
hsa-miR-3613-3p	ocu-miR-3613-3p	5`-ACAAAAAAAAAAGCCCAACCCUUC-3`

Table S6: Primer sequences used in this study

Target	Primer sequence
rat Gapdh-F	5`-GGGTGTGAACCACGAGAAAT-3`
rat Gapdh-R	5`-ACTGTGGTCATGAGCCCTTC-3`
rat Fgf10-F	5`-CCACATACATTTGCCTGCCG-3`
rat Fgf10-R	5`-GGGGAAACTCTATGGCTCAAAAG-3`
rat Vegfa-F	5`-AGAAAGCCCATGAAGTGGTGA-3`
rat Vegfa -R	5`-TCTCATCGGGGTACTCCTGG-3`
rat Flt1-F	5`-GTACCTCACCGTGCAAGGAA-3`
rat Flt1-R	5`-TTCGGAAGAAGACCGCTTCA-3`
rat Kdr-F	5`-CTGCAGGACCAAGGCAACTA-3`
rat Kdr-R	5`-CATGCGCTCTAGGATGACGA-3`
rabbit RPLP0-F	5`-CTGTGCCAGCTCAGAACACT-3`
rabbit RPLP0-R	5`-TGCACGTCGCTCAGGATTTC-3`
rabbit PLIN-2-F	5`-TGCTGAGCACATCGAGTCAC-3`
rabbit PLIN-2-R	5`-ATGTTGGACAGGAGGCTGTG-3`
rabbit BMP2-F	5`-GGAAGCTTTGGGAGACGACA-3`
rabbit BMP2-R	5`-TTTCGAGTTGGCTGTTGCAG-3`
rabbit BMP4-F	5`-CTTCCACCACGAAGAACATCTG-3`
rabbit BMP4-R	5`-ATGGCCTCGTTCTCTGGGAT-3`
rabbit Id1-F	5`-TTCTACAACCGTCTCCTGCG-3`
rabbit Id1-R	5`-CTGGCGACCTTCATGGTTCT-3`

Table S7: Details of antibodies used in this study

Target	Antibody	Company	Lung explants		Organoids		Primary epithelial cells	
			1°	2°	1°	2°	1°	2°
SPC	ab40879	Abcam (Cambridge, UK)	1:500	1:1,000	1:200	1:1,000	1:200	1:1,000
SOX9	HPA001758	SigmaAldrich (St Louis, MO)	1:500	1:1,000	-	-	-	-
Ki67	ab15580	Abcam (Cambridge, UK)	-	-	1:100	1:1,000	-	-
CC10	sc-365992	SantaCruz Biotechnology (Dallas, TX)	-	-	1:50	1:1,000	-	-
Vimentin	ab92547	Abcam (Cambridge, UK)	-	-	-	-	1:100	1:1,000

Target	Antibody	Company	Western Blot		ImmunoEM	
			1°	2°	1°	2°
TSG101	sc-7964	Santa Cruz Biotechnology, Dallas, TX	1:500	1:3,000	1:100	-
Goat-anti-mouse IgG (H&L)	25128 EM-grade 10nm gold tag	Electron Microscopy Sciences, Hatfield, PA	-	-	-	1:25
RNase	PA578151	Thermofisher Scientific, Waltham, Massachusetts	-	-	1:100	-
Goat-anti-rabbit IgG (H&L)	25116 EM-grade 25nm gold tag	Electron Microscopy Sciences, Hatfield, PA	-	-	-	1:25
CD63	EXOAB-KIT-1	System Biosciences, Palo Alto, CA	1:1,000	1:10,000	-	-
Flo-1	610820	BD Transduction Laboratories, San Jose, CA	1:1,000	1:3,000	-	-
Hsp70	EXOAB-KIT-1	System Biosciences, Palo Alto, CA	1:1,000	1:10,000	-	-

SPC: surfactant protein C,
SOX
9: SRY-Box 9,
Ki67: marker of proliferation Ki67,
CC10: Clara Cells 10 KDa Secretory Protein,
TSG101: Tumor susceptibility gene 101,

Flo-1: Flotillin 1,
Hsp70: Heat Shock Protein 70